processes

MDPI

Article

Filtration Experiments for Assessing EOR Efficiency in High-Viscosity Oil Reservoirs: A Case Study of the East Moldabek Field, Kazakhstan

Karlygash Soltanbekova [1,*], Gaukhar Ramazanova [1,*], Uzak Zhapbasbayev [1] and Zhenis Kuatov [2]

[1] Scientific and Production Laboratory "Energy Modeling", Satbayev University, Almaty 050013, Kazakhstan; uzak.zh@mail.ru
[2] Atyrau Branch of LLP "KMG Engineering", Atyrau 060097, Kazakhstan; zh.kuatov@kmge.kz
* Correspondence: soltanbekova.karlygash@mail.ru (K.S.); gaukhar.ri@gmail.com (G.R.)

Abstract: This study is dedicated to fundamental research on evaluating the effectiveness of enhanced oil recovery (EOR) methods for high-viscosity oil reservoirs. This paper presents the results of filtration experiments assessing the application of thermal, chemical, and gas-based EOR techniques to reservoir cores of high-viscosity oil, using the East Moldabek field in Kazakhstan as a case study. Experimental studies were conducted on the Cretaceous horizons M-II and M-III as well as the Jurassic horizon J-IV. The obtained production data from the East Moldabek wells indicated the low efficiency of conventional recovery methods. The objective of this study was to identify the most effective EOR method in terms of displacement efficiency. The investigated recovery techniques included base case conventional waterflooding (displacement using formation water), thermal EOR (hot-water flooding), chemical EOR (polymer flooding and ASP flooding), and gas EOR (nitrogen and CO_2 flooding). The filtration experiments were conducted at different times using various filtration systems. The results indicated that the most effective EOR methods for the highly viscous oil in the East Moldabek field were the chemical and thermal EOR techniques. The chemical EOR included ASP flooding, polymer flooding, and surfactant solution injection. ASP flooding achieved the highest increase in displacement efficiency, reaching 19%, making it the most effective method among all of the others.

Keywords: enhanced oil recovery (EOR); core flooding; thermal methods; chemical methods; gas methods; oil production; oil recovery; displacement efficiency; ASP flooding; interfacial tension

check for updates

Academic Editor: Qingbang Meng

Received: 6 March 2025
Revised: 27 March 2025
Accepted: 28 March 2025
Published: 3 April 2025

Citation: Soltanbekova, K.; Ramazanova, G.; Zhapbasbayev, U.; Kuatov, Z. Filtration Experiments for Assessing EOR Efficiency in High-Viscosity Oil Reservoirs: A Case Study of the East Moldabek Field, Kazakhstan. *Processes* **2025**, *13*, 1069. https://doi.org/10.3390/pr13041069

Copyright: © 2025 by the authors. Licensee MDPI, Basel, Switzerland. This article is an open access article distributed under the terms and conditions of the Creative Commons Attribution (CC BY) license (https://creativecommons.org/licenses/by/4.0/).

1. Introduction

Currently, numerous studies [1–11] worldwide are dedicated to searching for and selecting effective enhanced oil recovery (EOR) methods. Countries such as China, Canada, and India have extensive experience in applying chemical EOR techniques [12–15]. Thermal EOR methods have been widely employed in the United States, Oman, China, Canada, and Indonesia [16–21]. Additionally, Venezuela, Russia, Kazakhstan, Mexico, Colombia, and India have significant experience in thermal EOR applications [22–25]. Gas-based EOR is predominantly used in countries such as the United States, Brazil, and Canada [26–28]. In the United States, CO_2 injection has become widespread due to the availability of natural CO_2 sources. This method has demonstrated high efficiency, particularly in carbonate formations with low permeability/injectivity [26]. According to recent research, CO_2 injection contributed to an oil recovery increase of approximately 273,000 barrels per day in the U.S. in 2020 [5].

Chemical EOR is based on two primary mechanisms: improved macroscopic and microscopic displacement efficiency. The macroscopic efficiency of EOR can be enhanced through polymer flooding, wherein the injection of a polymer solution increases the viscosity of the displacing fluid and reduces its effective permeability with respect to water [25,29,30]. The microscopic displacement efficiency can be improved through the injection of alkalis and surfactants utilizing several mechanisms such as interfacial tension reduction, oil–water emulsification, the solubilization of interfacial films, wettability alteration, etc. The efficiency of the various methods of oil recovery varies greatly, as it depends on both the reservoir fluids and rock properties, including the reservoir pressure and temperature [29]. The economic performance of EOR is influenced by oil prices, the cost per barrel of injected solution, and the duration of chemical reagent injection [25].

Chemical EOR projects have been implemented across various oil fields worldwide. The largest application of chemical enhanced oil recovery is in China, where available data indicate that there has been an oil production increase of 300,000 barrels per day. Other countries that have adopted chemical EOR techniques to a significant extent include the United States and Canada. Polymer flooding and ASP flooding have been the most widely used chemical methods for clastic reservoirs [12].

In India, chemical EOR was first applied in the Sanand field [22]. Polymer flooding yielded promising results, achieving an incremental oil recovery of 23% of the initial oil in place (OOIP) [24]. Another major polymer-flooding project, entailing the development of existing fields, is the one that was carried out in the Mangala field. Initially, a pilot polymer-flooding project was launched, leading to a reduction in the water cut, followed by the implementation of an ASP flooding project [23].

To enhance oil recovery in Indonesia, several laboratory studies and field trials of chemical EOR methods have been conducted in fields such as the Minas, Tanjung, and Kaji Semoga fields, among others [31]. It has been estimated that chemical EOR methods can potentially recover an additional 2.48–4.90 billion barrels of oil.

In Kazakhstan, pilot tests of chemical EOR have been carried out in the North Buzachi, Kalamkas, Uzen, Zaburunje, and East Moldabek fields. Laboratory studies using core samples from Kazakhstani fields have demonstrated the effectiveness of chemical EOR methods [29,32].

The primary objective of the thermal EOR methods is to introduce a heat carrier into the reservoir to reduce oil viscosity, thereby improving the phase mobility in porous media and enhancing the recovery of oil. The main thermal EOR techniques that are used worldwide include steam injection, cyclic steam stimulation, in situ combustion, and SAGD (steam-assisted gravity drainage), which are considered conventional thermal recovery methods [17–19].

Thermal recovery techniques—particularly steam injection—continue to dominate as the most preferred enhanced oil recovery (EOR) method for heavy oil reservoirs [33].

Gas-based EOR is one of the most effective methods for enhancing oil recovery, and is widely applied internationally. The process of gas vaporization is used to improve reservoir oil recovery. In this method, gas slugs are injected into the reservoir to increase pressure; then, the gas dissolves in the reservoir oil, reducing its viscosity and enhancing its mobility under reservoir conditions. Industrial trials have shown that, at high pressures, nearly all of the components of crude oil can dissolve in the gas, except for resins and other heavy fractions [26–28]. When the pressure decreases at the surface, the gas, saturated with oil vapors, condenses into a liquid phase, forming a valuable condensate. Thus, the fundamental principle of this method is the artificial transformation of an oil reservoir into a gas-condensate reservoir.

Numerous efficient reservoir development technologies utilizing gas-based EOR methods are widely applied worldwide. These include high-pressure gas injection (using hydrocarbon gases, nitrogen, or flue gases), water alternating gas (WAG) injection, and carbon dioxide (CO_2) injection [4,5].

In gas-condensate reservoirs, offshore fields, and remote oil fields that lack access to gas markets, gas injection methods remain the preferred approach.

This study presents the results of a series of experiments conducted on core samples from the East Moldabek field to determine the greatest oil displacement efficiency that can be achieved with the tested EOR methods. Similar filtration experiments conducted on core samples using chemical agents have been reported in previous studies [34–36].

The geological and physical structures of the East Moldabek field's productive reservoirs are complex, featuring weakly cemented rock formations, gas–oil zones, a low initial reservoir pressure, and high-viscosity oil. Experimental studies were conducted on the Cretaceous horizons M-II and M-III as well as the Jurassic horizons J-IV, J-V, J-VI, and J-VII. Well performance data from the East Moldabek field indicate the low efficiency of conventional recovery methods in this field.

The East Moldabek field is located in the southeastern part of the Pre-Caspian Basin, in the interfluve of the Sagiz and Emba rivers.

In the Lower Cretaceous section of the productive formation, one gas–oil horizon (M-I) and two oil horizons (M-II and M-III) have been identified. The Middle Jurassic section contains seven productive horizons: J-I and J-II are gas–oil horizons, while J-IV, J-V, J-VI, and J-VII are oil-bearing horizons.

The depth of the horizons ranges from 190 to 810 m. The oil column in the Lower Cretaceous deposits varies between 35 and 57 m, while the gas column ranges from 1.4 to 16 m. Oil–water contact has been recorded at depths between 181 and 544 m. The reservoirs are stratified, anticlinal, and tectonically sealed. The productive horizons are composed of clastic rocks with porous-type reservoirs. The oil-saturated thickness ranges from 1.4 to 19.4 m, while the gas-saturated thickness varies between 1 and 14.6 m. The open porosity of the reservoirs is between 29% and 40%, with the permeability of the reservoirs ranging from 0.026 to 0.75 μm^2. The degree of oil saturation ranges from 0.56 to 0.77, and the degree of gas saturation ranges from 0.48 to 0.64.

The reservoir pressure ranges from 2.4 to 4.5 MPa, with temperatures between 23 °C and 27 °C.

The oils from the Cretaceous horizons are heavier than those from the Jurassic horizons but exhibit similar physicochemical properties. The density of the Cretaceous oils ranges from 891 kg/m^3 to 930 kg/m^3. These oils have a low sulfur content (0.23–0.48%), are resinous (6.02–14.8%), and have a low paraffin content (0.12–1.09%). The oil saturation pressure at reservoir temperature varies from 1.44 to 1.8 MPa, while the dynamic viscosity of the reservoir oil ranges from 74.1 mPa·s to 242 mPa·s.

The density of the Jurassic oils ranges from 877 to 898 kg/m^3. These oils have low sulfur (0.3–0.48%) and paraffin contents (0.13–2.36%). The resin content varies between 0.12% and 0.49%.

This study examines various reservoir stimulation methods, including the base method—oil displacement using formation water; thermal EOR—the injection of hot water; chemical EOR—polymer and ASP flooding; and gas EOR—nitrogen and CO_2 injection.

2. Equipment and Preparation of the Core, Formation Water, and Oil Samples for Experiments

For this study, both packed and drilled core samples were used, obtained from wells in the Cretaceous and Jurassic horizons of the East Moldabek field. For the Cretaceous

horizon M-I, packed core samples with a diameter of 38 mm (1.5 inches) and a length of approximately 5.8 cm were used. The sampling depth was 197 m. The core samples were manually collected and subsequently placed in special filtration containers, with the weight of each sample being no less than 100 g. For the Jurassic horizon J-IV, drilled core samples were used.

The core samples were cleaned using a Soxhlet apparatus along with organic solvent washing (Figure 1). A benzene–alcohol mixture was used as the solvent. The operating principle of the Soxhlet apparatus is straightforward: solvent vapors pass through a side tube into the extractor and, subsequently, the condenser, where they condense into liquid form, filling the container that holds the samples inside the extractor.

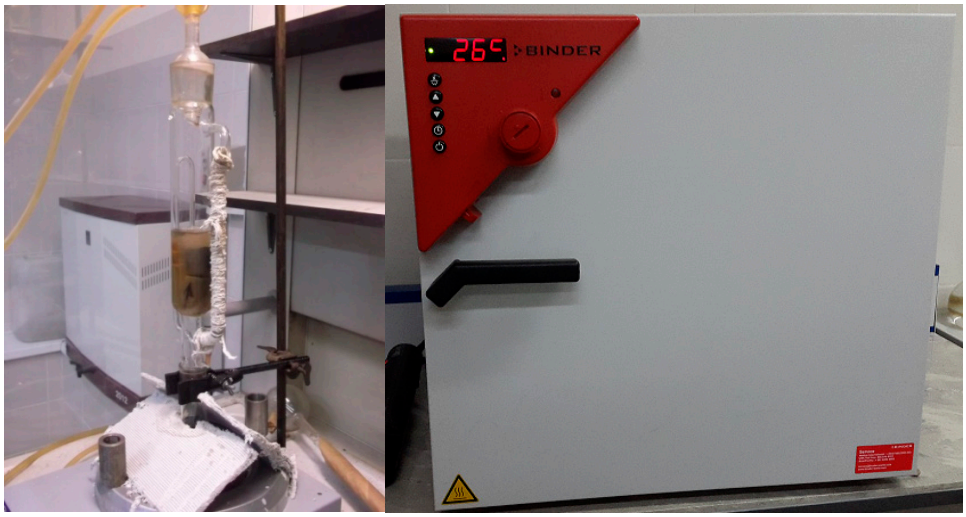


Figure 1. Soxhlet apparatus and drying oven used to wash and dry the core samples.

During the cleaning process, the samples were checked for luminescence under ultraviolet light. Combined with the color of the solvent, this procedure was used to determine the degree of hydrocarbon removal.

After undergoing complete cleaning, all of the samples were dried in a drying oven (DKN 600) at 60 °C until they reached a constant weight.

After ascertaining the basic volume and weight parameters of the samples, they were placed in a glass desiccator to reduce their adsorption of atmospheric moisture and then transferred for further standard analysis (i.e., the determination of porosity and gas permeability).

To determine the filtration and reservoir properties of the samples, the "Abacus" computerized workstation was used to conduct automated data entry regarding thee weight and dimensions of the samples. The results of sample weighing, performed on analytical scales with an accuracy of 0.001 g, and the average sample dimensions, measured using a digital caliper, were automatically recorded in a specially created table.

To measure the grain volume of the samples, a calibrated helium porosimeter (ULTRA-PORE 300) operating based on Boyle's law was used.

The absolute permeability of the samples was measured using gas (nitrogen) with calibrated ULTRA-PERM 600 equipment, which was equipped with the latest mass flow meters and pressure sensors. This software performs calculations using Darcy and Klinkenberg equations to determine the gas permeability of samples and the inverse of the mean pressure.

The fundamental Darcy equation for calculating gas permeability is as follows:

$$K_g = \frac{2000 \cdot P_1 \cdot \mu \cdot Q_1 \cdot L}{(P_1^2 - P_2^2) \cdot A} \quad (1)$$

where K_g is the gas permeability, mD; μ is the gas viscosity, cP; Q_1 is the gas flow rate, cm^3/s; P_1 is the inlet pressure, atm; P_2 is the outlet pressure, atm; A is the cross-sectional area of the sample, cm^2; and L is the sample's length, cm.

For conducting the special filtration studies, the PLS-200 system with four hydrostatic core holders was used (Figure 2). The core holders were configured to operate under pressures of up to 10,000 psi and temperatures of up to 150 °C to closely simulate reservoir conditions.

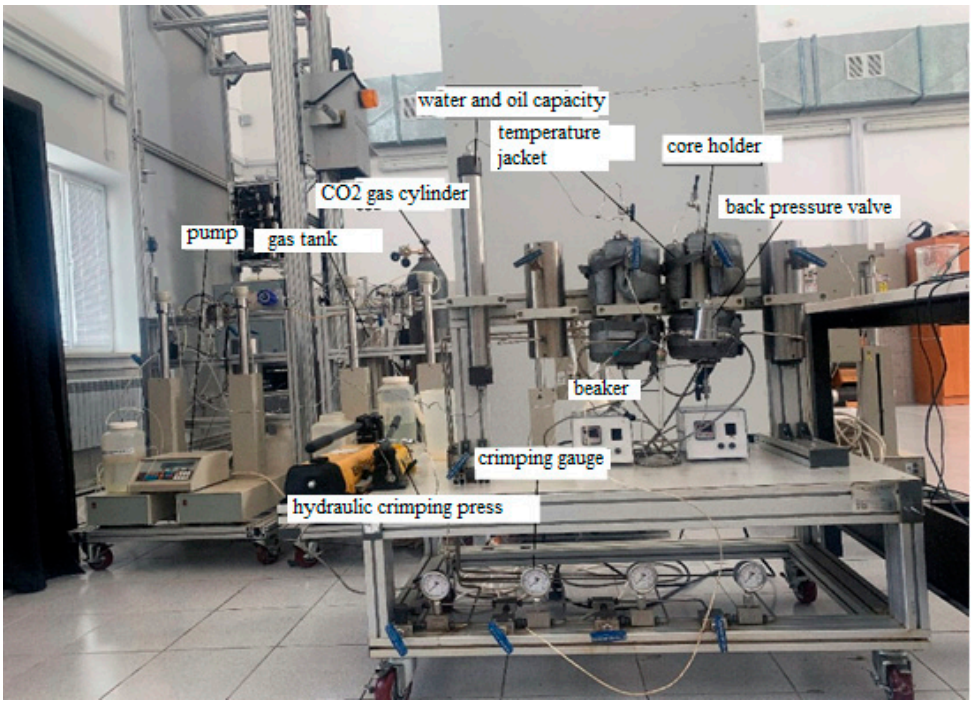


Figure 2. PLS-200 filtration system.

The device is equipped with a pulse-free piston pump capable of injecting water, oil, and polymer at up to 3650 psi at flow rates ranging from 0.001 to 204 mL/hour. Additionally, it includes a DPS-100 differential pressure measurement system with two high-precision sensors (0.05%).

The core samples were initially saturated with formation water and then placed into the hydrostatic core holders of the system. An automatic saturator (AST-600) was used to saturate the model samples with water, allowing for the automated selection of the air evacuation time and saturation pressure, and thus ensuring fast and complete saturation of the core samples.

For the injection of water, oil, and polymer during the filtration studies, high-pressure dual-cylinder pulse-free syringe pumps and cylindrical piston displacement containers were used.

All filtration experiments were conducted without using back pressure, as the fluid output volumes were calculated using the material balance method. During each experiment, the core holders were wrapped with special heating jackets to maintain the reservoir temperature: 19.7 °C for the Cretaceous horizon and 29.3 °C for the Jurassic horizon.

2.1. Methodology for Filtration Studies on Core Samples

1. The samples were 100% saturated with formation water, and their water permeability (kw) was determined: the water permeability of the sample (k), before any interaction between the injected water, the formation water, and the rock in its pore channels, was calculated using Darcy's formula in three different flow regimes.

$$k = \frac{0.1Q\mu L}{tF\Delta P}$$

where k is the water permeability of the core sample, μm^2; Q is the volume of formation water passing through the core sample, cm^3; μ is the water viscosity, mPa·s; L is the length of the core sample, cm; t is the water filtration time, s; F is the cross-sectional area of the core sample, cm^2; and ΔP is the pressure drop at the end of the core sample, MPa;

2. The water in the samples was displaced by oil, and the residual water saturation (Swi) was determined in order to simulate reservoir conditions;
3. The samples were saturated with oil;
4. The oil in the samples was displaced with technical water: graduated cylinders were placed at the outlet tubes from the core holder to measure the amount of recovered oil, which was later used to determine the oil recovery factor. The efficiency with which the oil was displaced by the water was calculated as the ratio of the displaced oil volume V_o to the initial oil volume before the injection of the displacement agent $V_{init\ o}$:

$$\beta = \frac{V_o}{V_{init\ o}}$$

5. After injecting 7–8 pore volumes into the core and increasing the water cut in the produced fluid to 95–99%, the selected displacement agent (alkali/surfactant, polymer, hot water, nitrogen, or carbon dioxide) was injected until the pressure differential stabilized.

In some of the filtration studies, the pumped volume was used, instead of the Vinj water/Vpore ratio, to plot the graph of the displacement efficiency coefficient.

In all cases of polymer flooding, the FloPaam 5205 VHM polymer was used in concentrations of 2000, 2500, and 3000 ppm, along with the heat-resistant polymer TR-15-16.

2.2. Object of Study for Filtration Experiments

Core Material: Core material from the Cretaceous and Jurassic horizons was used for filtration studies. The baseline data for the filtration experiments conducted on the core samples are presented in Table 1. For some samples, the exact core sampling depth was unknown. It is known that the reservoir's filtration and storage properties are heterogeneous, as shown in Figure 3. A significant variation in the absolute permeability values with depth and as a function of porosity can be observed (Figure 3).

Table 1. Initial data for the core material.

No. of the Core Sample Model	Experimental Group, EOR Method	Horizon	Sampling Depth, m	Porosity, %	Gas Permeability, mD
1	ASP flooding	Cretaceous	258.75	36.76	1460
2		Cretaceous	260.65	36.853	1300
3		J-IV	496.8	32.261	92.3
4		J-IV	497.25	33.681	127.7

Table 1. *Cont.*

No. of the Core Sample Model	Experimental Group, EOR Method	Horizon	Sampling Depth, m	Porosity, %	Gas Permeability, mD
5	Surfactant solution flooding	J	-	29.69	430
6	Polymer flooding	J	-	30.48	271
7	Polymer flooding	J-IV	497.3	32.08	3267
8	Polymer flooding	J-IV	498.47	30.47	1290
9	Thermal effects	J-IV	496.9	31.48	1623
10	Thermal effects	J	-	32.65	259.8
11	Thermal effects	J	-	28.917	341
12	Thermal effects	J	-	29.299	1000
13	N_2 (nitrogen) injection	Cretaceous	197.35	38.14	174.3
14	CO_2 (carbon dioxide) injection	Cretaceous	197.20	37.83	242.1

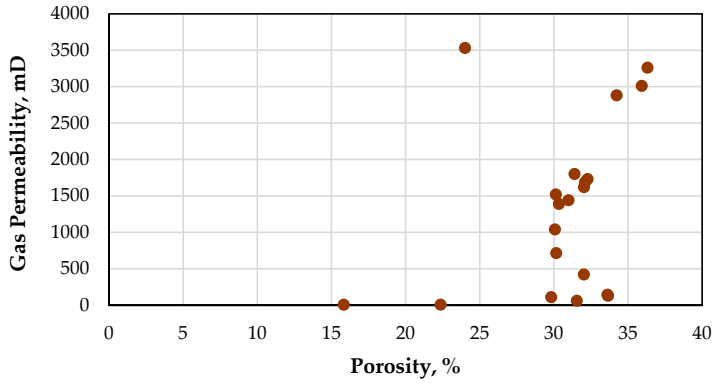


Figure 3. Reservoir properties of the core material.

Oil: Crude oil samples from various wells and horizons were used for the filtration studies. At temperatures of 25–35 °C, the oil behaves as a pseudoplastic fluid, while, at higher temperatures, it exhibits Newtonian behavior. Figure 4 illustrates the dependence of the viscosity of the Jurassic horizon (J-IV) oil on the temperature.

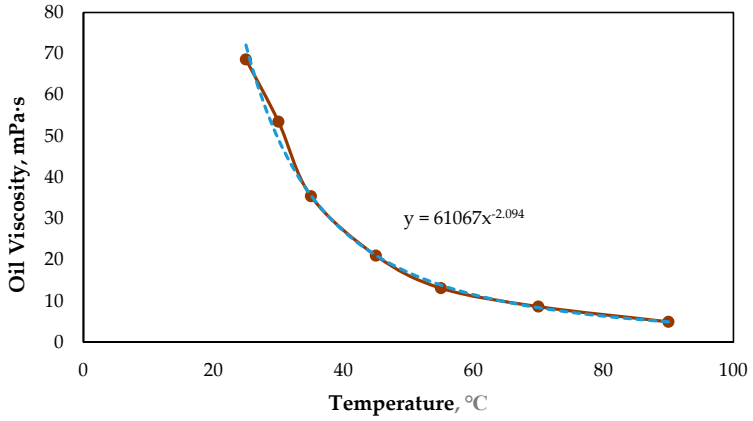


Figure 4. J-IV horizon oil viscosity at different temperatures.

Formation Water: For the filtration experiments, the formation water of the Moldabek East field was simulated under laboratory conditions with a salinity of 173 g/L. One liter of synthetic water contains the following ions: HCO_3—0.195 g; SO_4—0.793 g; Cl—104.6 g; Ca—1.9 g; Mg—0.79 g; and Na + K—64.6 g.

The physical properties of the formation water are presented in Table 2.

Table 2. The physical properties of the technical and formation water.

No.	Name	Density, g/cm³	Viscosity, mPa·s
1	Formation water (Cretaceous horizon)	1.0756	1.3
2	Formation water (Jurassic horizon)	1.0926	1.32
3	Technical water	1.0908	1.1

Polymer Flopaam 5205VHM (SNF Floerger, Andrézieux-Bouthéon, France): The concentration range for the industrial application of this polymer is 0.1–0.5% g/L of formation water. Figure 5 presents the rheological curves of Flopaam 5205VHM at different temperatures.

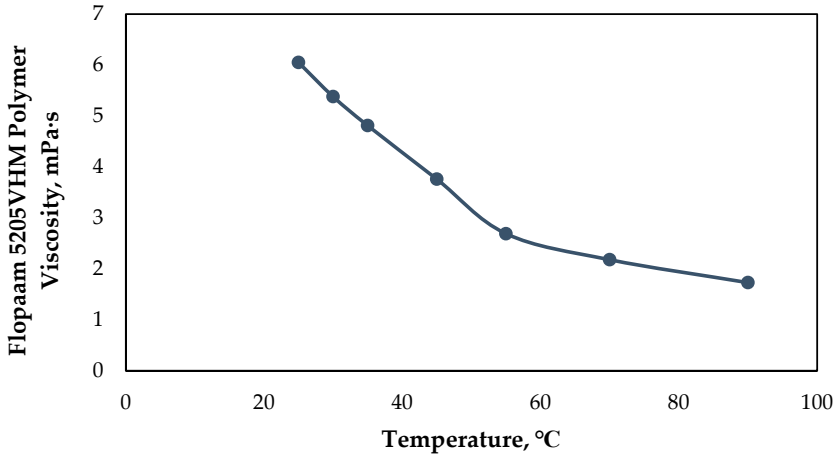


Figure 5. Dependence of the viscosity of the polymer Flopaam 5205VHM solution (0.1 wt.%) on temperature.

At temperatures below 55 °C, Flopaam 5205VHM exhibits pseudoplastic behavior, whereas, at higher temperatures, it behaves as a Newtonian fluid. The upper temperature limit for the applicability of this polymer, as recommended by the manufacturer, is 50 °C. When overheated, the polymer undergoes degradation, which significantly reduces its pseudoplastic properties and decreases its viscosity.

Polymer TR-15-16 (SNF Floerger, France): This polyacrylamide can be used in reservoirs with temperatures of up to 90 °C. The concentration range for its industrial application is 0.1–0.5% g/L of formation water. Figure 6 illustrates the dependence of TR-15-16's viscosity on the temperature. The polymer exhibits pseudoplastic behavior across the entire studied temperature range. Figure 7 illustrates the viscosity ratio of oil to the different displacing agents used. Notably, both polymers exhibit highly similar viscosity characteristics across the entire temperature range.

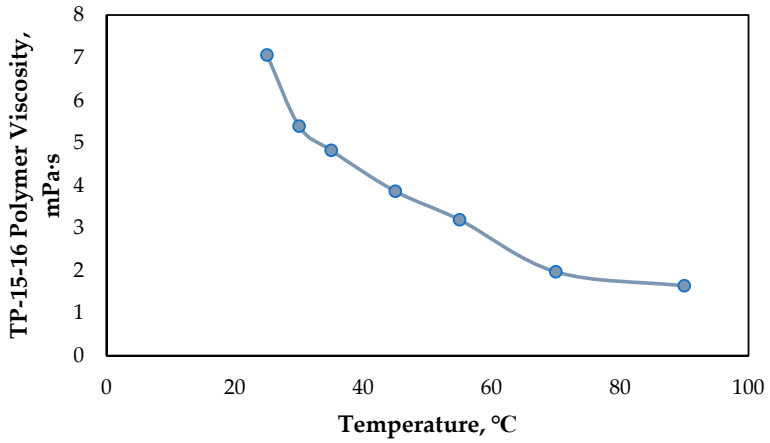


Figure 6. Dependence of the viscosity of TR-15-16 aqueous solution (0.1 wt.%) on temperature.

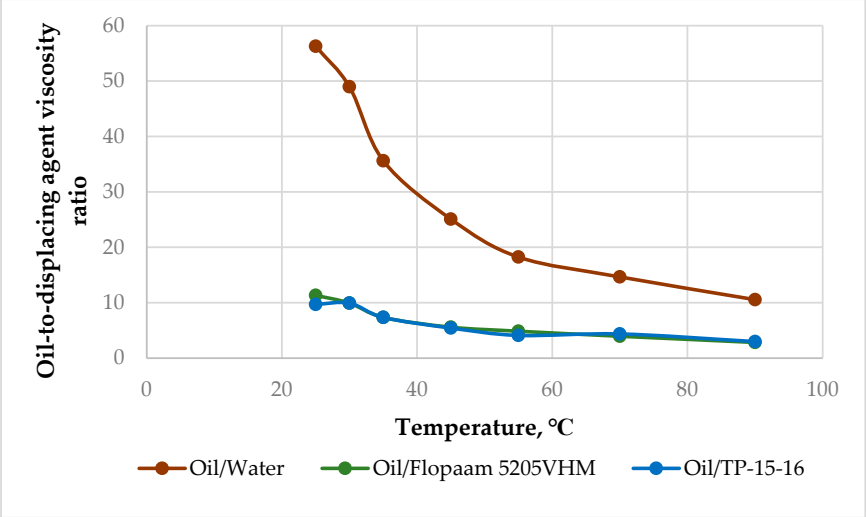


Figure 7. Oil—displacing agent viscosity ratio at different temperatures.

The key differences between the two polymers are presented in Table 3.

Table 3. Differences between the polymers Flopaam 5205VHM and TR-15-16.

Property	Flopaam 5205VHM	TR-15-16
Thermal stability	Up to 60 °C	Up to 90 °C
Water salinity	Sensitive	More resistant
Solution viscosity	High, but degrades at high temperatures	Stable at high temperatures

3. Results of Experimental Studies

3.1. Filtration Experiment Results for Chemical EOR

The results of the analysis of standard core samples from the East Moldabek field are summarized in Table 4, demonstrating the effectiveness of the ASP flooding method (using alkali, surfactant, and polymer agents).

Table 4. Results of the standard core sample analysis.

No.	Sampling Depth, m	Length, cm	Diameter, cm	Porosity, %	Gas Permeability, mD	
1	258.75	5.854	3.822	36.76	1460	packed
2	260.65	5.732	3.809	36.853	1300	packed
3	496.8	5.856	3.808	32.261	92.3	drilled
4	497.25	5.981	3.813	33.681	127.7	drilled

3.2. ASP Flooding

The ASP flooding filtration experiments were conducted as follows:

1. Steps 1–5 were carried out according to the core sample filtration testing methodology;
2. After 7–8 pore volumes were injected into the core and a water cut of 95–99% was reached in the produced fluid, a selected alkaline/surfactant solution was injected in an amount of 1–1.5 mL of the pore volume (Table 5);
3. A polymer solution was then injected until the water cut reached 99% and pressure stabilization was achieved to determine the resistance factor. The resistance factor (R_f) is defined as the ratio of the permeability of the core to mineralized water (λ_w) to the permeability of the core to a single-phase polymer solution (λ_p) under identical conditions:

$$R_f = \frac{\lambda_w}{\lambda_p}$$

4. After the polymer solutions were injected into the core, the polymer was replaced with technical water. The core was then flushed with technical water until pressure stabilization was achieved, and then the residual resistance factor was calculated. The residual resistance factor serves as a key indicator of whether flow channels are blocked due to the application of the polymer solution. The residual resistance factor (R_{rf}) is determined by the ratio of the water mobility before (λ_w) to that after polymer injection (λ_{w2}):

$$R_{rf} = \frac{\lambda_w}{\lambda_{w2}}$$

Phase behavior tests at the alkali/surfactant–oil interface.

Lauryl sulfate (hereinafter referred to as the surfactant) was used as a surfactant, while sodium hydroxide was used as the alkali agent. These reagents were prepared in the required concentrations using technical water and were mixed until fully dissolved.

Based on the results of the phase behavior tests conducted at different alkali and surfactant concentrations, the following concentrations were selected for the filtration studies.

1. Using Cretaceous horizon water:
   a. 0.02% surfactant and 0.8% alkali;
   b. 0.02% surfactant and 0.6% alkali.
2. Using Jurassic horizon water:
   a. 0.02% surfactant and 0.8% alkali;
   b. 0.02% surfactant and 0.6% alkali;

The specific alkali/surfactant concentrations for each experiment are presented in Table 5.

The experimental conditions and the results of the filtration experiments conducted to determine the oil displacement efficiency when using the ASP agent are presented in Table 5 and Figure 8.

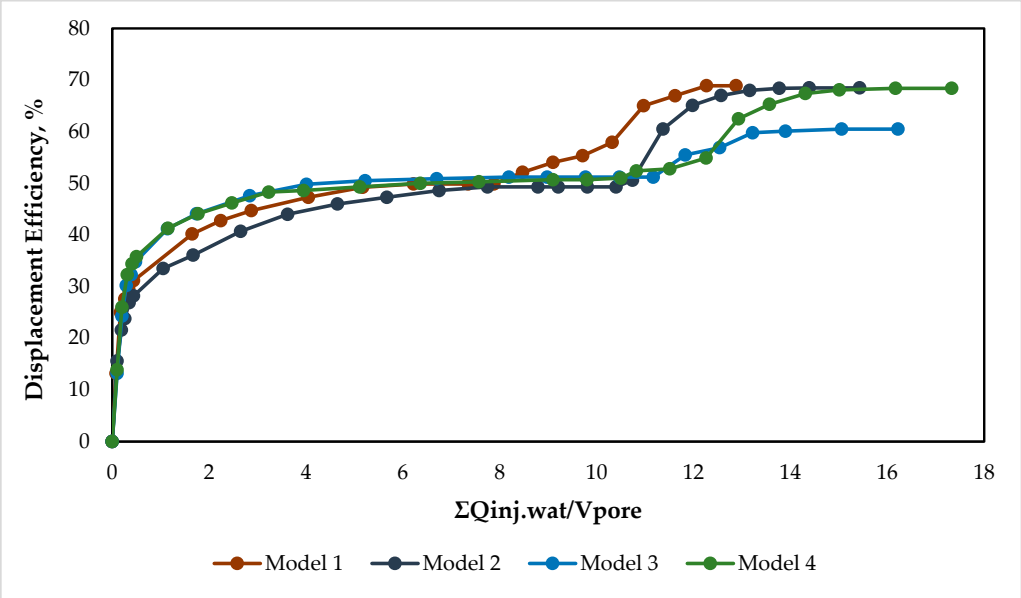


Figure 8. Core-flooding results for oil displacement using an ASP agent.

Table 5. Filtration experiment results for assessment of the oil displacement efficiency of an ASP agent.

Name	Value			
Results of Standard Core Sample Studies				
No. of the Core Sample Model	Model 1	Model 2	Model 3	Model 4
Horizon	Cretaceous	Cretaceous	J-IV	J-IV
Sampling Depth, m	258.75	260.65	496.8	497.25
Diameter, cm	5.854	5.732	5.856	5.981
Porosity, %	36.76	36.853	32.261	33.681
Gas Permeability, mD	1460	1300	92.3	127.7
Experimental Conditions				
EOR Method	ASP Flooding			
Temperature, °C	20	19.7	29.3	29.3
Oil Viscosity Under Experimental Conditions, mPa·s	407.4	407.4	66.1	66.1
Water Viscosity Under Experimental Conditions, mPa·s	1.05	1.1	1.1	1.1
Polymer Concentration, ppm	2500	3000	2000	3000
Alkali/Surfactant Concentration, g	0.02/0.8	0.02/0.6	0.02/0.6	0.02/0.8
Results of the Experiments				
Displacement Efficiency After Waterflooding, %	49.9	49.3	51.2	50.7
ASP Flooding Displacement Efficiency, %	68.9	68.5	60.5	68.4
Residual Oil Saturation After Polymer Injection, fraction	0.2	0.199	0.26	0.211
Increase in Displacement Efficiency, %	19	19.2	9.3	17.7

As shown in Table 5, which summarizes the filtration experiment results for the ASP flooding, the highest increase in the displacement efficiency coefficient was achieved using the higher-viscosity oil. Specifically, for the oil from the Cretaceous horizon with a viscosity of 407.4 mPa·s, the additional increase was 19.2%, which can be compared to that of 17.7% for the oil from the Jurassic horizon with a viscosity of 66.1 mPa·s. However, it should

be noted that the gas permeability in the Cretaceous horizon is significantly higher than that in the Jurassic horizon (see Table 4)—1460 mD versus 127.7 mD. Additionally, the core samples from the Cretaceous horizon were packed samples.

These filtration experiment results indicate that ASP flooding is an effective enhanced oil recovery (EOR) method for high-viscosity oil. Overall, as shown in the graph (Figure 8), in most cases, the displacement efficiency reached 68%.

3.3. Injection of Surfactant and Polymer Solutions

The results of the filtration experiment conducted to determine the oil displacement efficiency during the injection of surfactant and polymer solutions are presented in Table 6.

Table 6. Results of the filtration experiment conducted to determine the oil displacement efficiency during the injection of the surfactant and polymer solutions.

Name	Value	
Results of Standard Core Sample Studies		
No. of the Core Sample Model	Model 5	Model 6
Horizon	J	J
Diameter, cm	5.854	5.732
Porosity, %	29.69	30.48
Gas Permeability, mD	430	271
Experimental Conditions		
EOR method	Surfactant solution flooding	Polymer flooding
Temperature, °C	30	30
Oil Viscosity Under Experimental Conditions, mPa·s	96	96
Water Viscosity Under Experimental Conditions, mPa·s	1.05	1.1
Results of the Experiments		
Displacement Efficiency After Waterflooding, %	25.89	27.0
Displacement Efficiency After Displacement Agent Flooding, %	35.29	39
Increase in Displacement Efficiency, %	9.4	12

The core pore volume was 6.471 cm^3 (porosity: 29.69%), and the absolute air permeability was 430 mD.

Throughout the entire experiment, core saturation and subsequent water flooding were achieved using formation water at a flow rate of 0.1 cm^3/min.

A total of seven pore volumes of formation water and surfactant solution were injected into the core. The first two pore volumes of formation water were injected to simulate conventional waterflooding at a reservoir temperature of 30 °C. At the end of the waterflooding, the displacement efficiency reached 25.89%.

To simulate a chemical flooding method, two types of surfactants—Surfactant 1 (S1) and Surfactant 2 (S2)—were used in this experiment. To evaluate their oil displacement efficiencies, each surfactant solution was injected separately in a quantity of two pore volumes. After injecting a total of five pore volumes of S1 and S2, the additional increases in the displacement efficiency were 8.4% and 1%, respectively. The overall displacement efficiency for the core (Figure 9, Model 5) reached 35.29% (Figure 9).

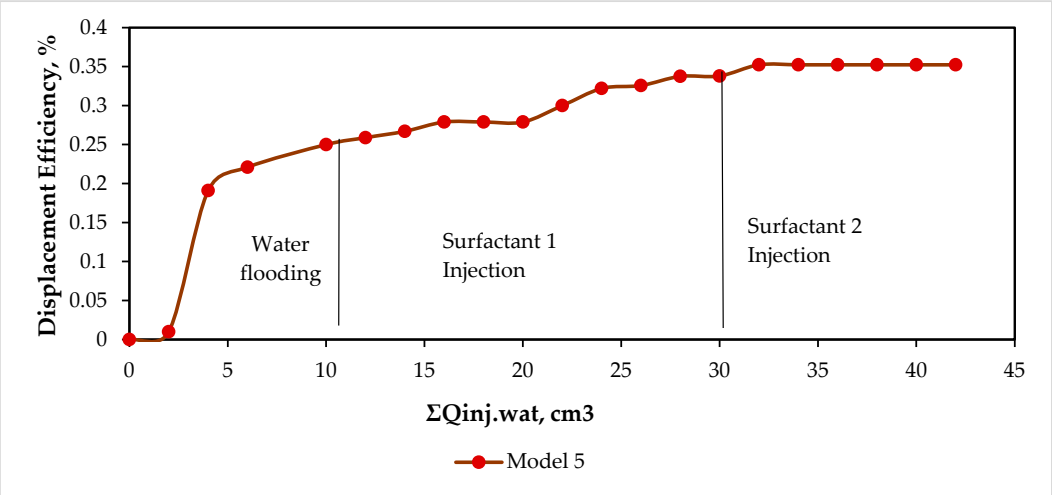


Figure 9. Core flooding results for surfactant solution injection (Model 5).

For the polymer flooding, conventional waterflooding was first simulated by injecting three pore volumes of formation water into the core (Figure 10, Model 6). The absolute permeability of core Model 6 was 271 mD. The core pore volume was 6.457 cm^3 (porosity: 30.48%). Throughout the experiment, core saturation and subsequent water flooding were achieved using formation water at a flow rate of 0.1 cm^3/min.

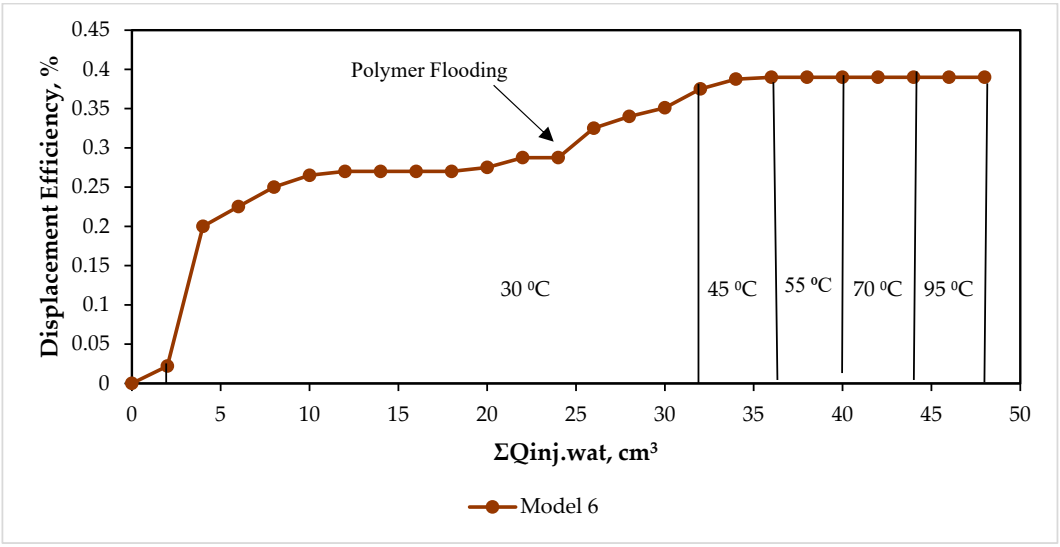


Figure 10. Core flooding results for polymer solution injection and thermal treatment (Model 6).

The oil displacement efficiency for the water injection was 27%, with flooding carried out at a temperature of 30 °C. Subsequently, a 0.1% solution of partially hydrolyzed polyacrylamide (HPAM) with a degree of hydrolysis of 30% and a molecular weight of 18×10^6 was injected. The first two pore volumes of HPAM solution were injected at 30 °C, and then the temperature was gradually increased to 95 °C (Figure 10).

3.4. Results of Filtration Experiments Involving Polymer Flooding

The results regarding the displacement of oil by an aqueous solution of Flopaam 5205 VHM and TP-15-16 polymers under constant pressure-drop conditions are shown in Figure 11 (Table 7). Under four-pore-volume injection, the permeability of the core for the polymer solution reached 1.36 mD.

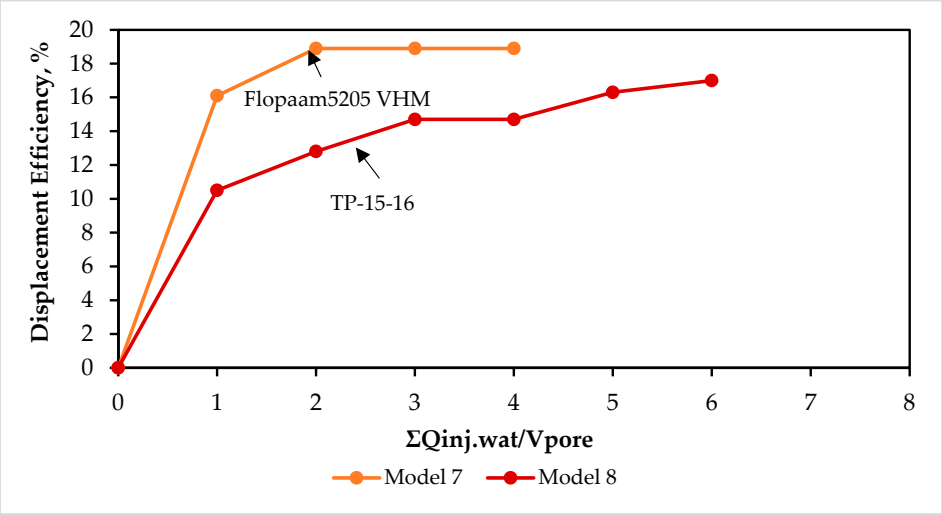


Figure 11. Core-flooding results: oil displacement by an aqueous solution of Flopaam 5205 VHM polymer (Model 7), and oil displacement by a heat-resistant polymer solution, TP-15-16, with additional thermal treatment (Model 8).

Table 7. Results of the filtration experiment conducted to determine the oil displacement efficiency during polymer flooding.

Name	Value		
Results of Standard Core Sample Studies			
No. of the Core Sample Model	Model 7	Model 8	
Horizon	J-IV	J-IV	
Porosity, %	32.08	30.47	
Gas Permeability, mD	3267	1290	
Experimental Conditions			
Oil Viscosity Under 30 °C, mPa·s	95	96	
Initial Water Saturation Degree, fraction	0.22	0.169	
Initial Oil Saturation Degree, fraction	0.78	0.831	
Results of the Experiments			
EOR method	Flopaam5205 VHM polymer flooding	TP-15-16 polymer flooding	
Displacement Efficiency After Waterflooding at a Temperature of 30 °C, %	18.9	12.8	14.7
Displacement Efficiency After Waterflooding at a Temperature of 35 °C, %			
Displacement Efficiency After Waterflooding at a Temperature of 45 °C, %		15.5	
Displacement Efficiency After Waterflooding at a Temperature of 55 °C, %			
Displacement Efficiency After Waterflooding at a Temperature of 70 °C, %		17	
Displacement Efficiency After Waterflooding at a Temperature of 90 °C, %			
Increase in Displacement Efficiency, %	6	4.1	

A relatively rapid stabilization of the pore space saturation was observed. The aqueous solution of Flopaam 5205 VHM led to an increase in the displacement efficiency compared to the formation water at the same temperature (18.9% vs. 12.9%, respectively) (Table 7).

The displacement of oil by water in a volume of two pore volumes (T = 30 °C) was followed by additional displacement using a heat-resistant polymer solution, TP-15-16, at temperatures of 30, 45, and 70 °C. Figure 11 presents a graph of the displacement efficiency increase and permeability variation obtained with the displacing agent. The displacement efficiency during the water injection was 12.8%. During the additional oil displacement using the polymer solution, the displacement efficiencies achieved were 14.7%, 15.5%, and 17.0% at 30, 45, and 70 °C, respectively.

At equal concentrations, the polymer solution TP-15-16 was less effective than Flopaam 5205 VHM. The displacement efficiency for Flopaam 5205 VHM reached 18.9% (at reservoir temperature), whereas that for TP-15-16 was 17.0% (at 70 °C).

3.5. Results of Filtration Experiments on Thermal EOR Methods (Hot-Water Injection)

Two filtration experiments were conducted at different times to determine the displacement efficiency during thermal treatment using hot water.

The displacement of oil by water was studied at different temperatures: 25, 30, 35, 45, 55, 75, and 90 °C (Table 8). Figure 12 presents a graph of the increase in the displacement efficiency as a function of the water injection. The water injection rate remained constant at all temperatures. After 70 °C, the increase in the displacement efficiency declined, which may be attributed to the rheological properties of fluids: at temperatures above 70 °C, the viscosities of oil and water, as well as their viscosity ratios, change only slightly (Figure 12).

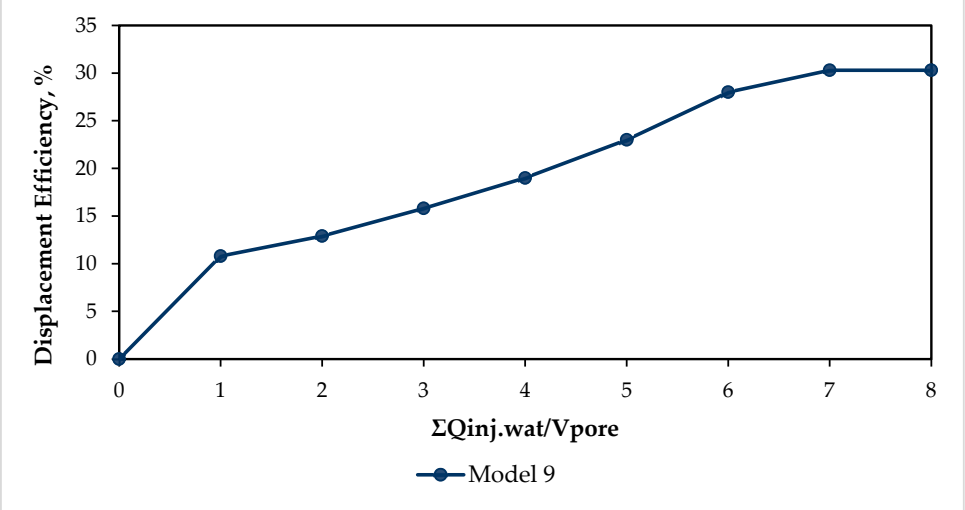


Figure 12. Results regarding core flooding during thermal treatment (Model 9).

A reduction in permeability (typically at 100% water saturation) during reservoir heating is usually associated with the thermal expansion of the rock matrix, the washing out of fine-grained fractions, and, consequently, the narrowing of pore channels. In our case, the saturation dynamically changed with heating; the water saturation increased, which should, theoretically, have a positive effect on the water permeability. However, it appears that, at high temperatures, the expansion of the rock matrix outweighed the effect of increased water saturation.

To simulate the thermal effects on the reservoir, water was injected into the core at elevated temperatures. The temperature in the core holder was gradually increased from 45 °C to 95 °C. A total of four pore volumes of formation water was injected into the

core. The first two pore volumes were injected to simulate conventional waterflooding at a reservoir temperature of 30 °C.

Based on the results of the thermal flooding—i.e., hot-water injection—the highest increase in the displacement efficiency was 8.75% at 95 °C for Model 1 (Figure 13, Model 10). The overall displacement efficiency in this case reached 49.58%. In the other two cases, the additional increase in displacement efficiency did not exceed 2.92% (Table 8, Figure 13), with the highest displacement efficiency being recorded at 53.36%. Compared to the other two experiments, Model 12 (Figure 13) exhibited a higher displacement efficiency after conventional waterflooding (52.1%) but a low displacement efficiency after thermal flooding (1.26%).

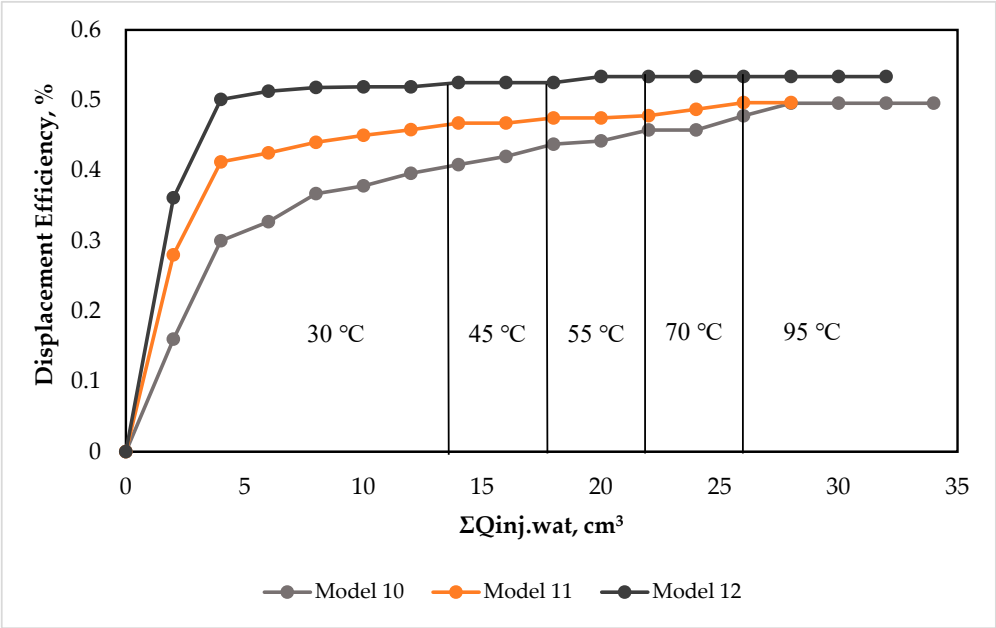


Figure 13. Results for core flooding during thermal treatment (Models 10–12).

Table 8. Results of the filtration experiment conducted to determine the oil displacement efficiency during thermal treatment.

Name	Value			
Results of Standard Core Sample Studies				
No. of the Core Sample Model	Model 9	Model 10	Model 11	Model 12
Horizon	J-IV	J	J	J
Core Sample Pore Volume, cm^3	-	7.046	6.282	6.385
Porosity, %	31.48	32.65	28.917	29.299
Gas Permeability, mD	1623	259.8	341	1000
Experimental Conditions				
EOR method	Thermal Effects			
Oil Viscosity Under 30 °C, mPa·s	75	96	116	21.4
Initial Water Saturation Degree, fraction	0.258	0.295	0.242	0.285
Initial Oil Saturation Degree, fraction	0.742	0.705	0.758	0.715

Table 8. *Cont.*

Name	Value			
Results of the Experiments				
Displacement Efficiency After Waterflooding, %	12.9	40.83	46.74	52.1
Displacement Efficiency After Waterflooding at a Temperature of 45 °C, %	19.0	43.74	47.47	52.1
Displacement Efficiency After Waterflooding at a Temperature of 55 °C, %	23.0	45.76	48.2	53.36
Displacement Efficiency After Waterflooding at a Temperature of 70 °C, %	28.0	47.78	49.66	53.36
Displacement Efficiency After Waterflooding at a Temperature of 90 °C, %	30.3	-	-	-
Displacement Efficiency After Waterflooding at a Temperature of 95 °C, %		49.58	49.66	53.36
Increase in Displacement Efficiency, %	17.4	8.75	2.92	1.26

3.6. Results of Filtration Experiments on Gas EOR Methods

Injection of Nitrogen and CO_2

The filtration experiments demonstrated that using nitrogen and carbon dioxide (CO_2) as displacement agents can enhance the oil displacement efficiency by mobilizing residual oil. Nitrogen injection increased the displacement efficiency to 36.2%, with an incremental increase of 3.6%. CO_2 injection resulted in a displacement efficiency increase of 5.06% compared to conventional waterflooding (Table 9, Figure 14). This effect can be attributed to the dissolution of the CO_2 in the oil, a process that reduces oil's viscosity and improves its flowability.

Table 9. Results of the filtration experiment conducted to determine the oil displacement efficiency during nitrogen and CO_2 injection.

Name	Value	
Results of Standard Core Sample Studies		
No. of the Core Sample Model	Model 13	Model 14
Horizon	Cretaceous	Cretaceous
Sampling Depth, m	197.35	197.20
Length, cm	6.05	5.80
Diameter, cm	3.83	3.83
Porosity, %	38.14	37.83
Gas Permeability, mD	174.3	242.1
Experimental Conditions		
EOR method	N_2 (Nitrogen) Injection	CO_2 (Carbon Dioxide) Injection
Temperature, °C	25	25
Oil Viscosity Under Experimental Conditions, mPa·s	358.0	358.0
Water Viscosity Under Experimental Conditions, mPa·s	1.4	1.4

Table 9. *Cont.*

Name	Value	
Results of the Experiments		
Residual Water Saturation (S_{wi}), fraction	0.321	0.375
Residual Oil Saturation After Waterflooding (S_{ow}), fraction	0.462	0.430
Displacement Efficiency Waterflooding, %	32.6	31.3
Displacement Efficiency After Displacement Agent Flooding, %	36.2	36.3
Increase in Displacement Efficiency, %	3.6	5.06

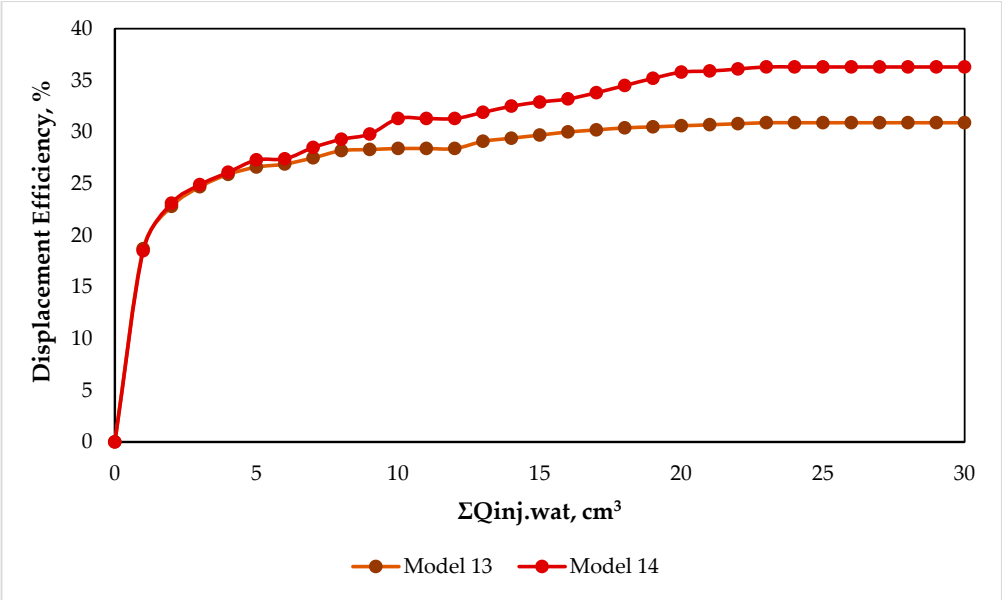


Figure 14. Core-flooding results for the displacement of oil by nitrogen (Model 13) and CO_2 (Model 14).

4. Conclusions

Our experimental studies included conducting filtration experiments on the displacement of highly viscous oil using core samples from the East Moldabek field to determine effective methods for enhancing oil recovery. The objective was to identify the most efficient enhanced oil recovery (EOR) method in terms of its displacement efficiency improvement. The tested methods included baseline displacement using formation water, thermal EOR through hot-water injection, chemical EOR via polymer flooding and ASP injection, and gas EOR using nitrogen and CO_2 injection.

Table 10 provides a summary of the advantages and disadvantages of the enhanced oil recovery (EOR) methods analyzed in this study.

Filtration experiments were conducted at different times using various filtration systems. The results indicated that the most effective EOR methods for the highly viscous oil in the East Moldabek field were chemical and thermal EOR techniques. The chemical EOR methods included ASP flooding, polymer flooding, and surfactant solution injection. ASP flooding achieved the highest increase in displacement efficiency, reaching 19%, making it the most effective method among all of the others.

Table 10. Summary of enhanced oil recovery (EOR) methods [1–3].

EOR Method	Advantages	Disadvantages	Economic Feasibility	Results of Filtration Experiments Regarding the Increase in EOR Displacement Efficiency, %
ASP Flooding	It significantly reduces interfacial tension, enhancing oil displacement. It is effective in reservoirs with high residual oil saturation. It works well in combination with polymers.	It allows high adsorption of chemicals on the rock. There is a potential for reactions with minerals, reducing efficiency. Challenges regarding compatibility with reservoir conditions can arise.	Average cost: USD 20–50 per additional barrel of oil. It is profitable when residual oil remains in heterogeneous reservoirs. Technical challenges: it requires careful chemical formulation adaptation.	19.2
Polymer Flooding	It increases water viscosity, improving oil displacement. It reduces water saturation and lowers the water cut in produced oil. It is highly suited to mature fields	Polymers may degrade at high temperatures and degrees of salinity. High polymer adsorption on the rock is possible. Injection challenges may occur in low-permeability reservoirs.	Average cost: USD 10–30 per additional barrel of oil. Iti s highly profitable when used in mature reservoirs with high water saturation. Limitations: it requires adaptation of composition to reservoir conditions (temperature, mineralogy, etc.).	12
Thermal Methods (Steam and Thermal Effects)	It enhances mobility of heavy oil. It enables deep reservoir penetration. It is suitable for bitumen and extra-heavy-oil recovery.	It incurs high energy consumption and steam generation costs. It offers limited efficiency in highly heterogeneous reservoirs. There is a potential environmental impact.	Average cost: USD 20–70 per additional barrel of oil. It is highly profitable for heavy oil but dependent on energy costs. It is best suited to bitumen sands and deep reservoirs.	17.4
Gas Injection (N_2, Natural Gas)	It improves reservoir pressure. It is suitable for low-permeability reservoirs. It works well in combination with other methods.	This gas has lower solubility in oil compared to CO_2. It leads to high gas losses due to breakthrough in production wells. It requires large gas volumes.	Average cost: USD 15–40 per additional barrel of oil. It offers limited profitability if natural gas is expensive. It is effective in gas caps but less versatile than CO_2-EOR.	3.6
CO_2 Injection (CO -EOR)	It reduces oil viscosity, improving mobility. It can be integrated with CO_2 capture and storage (CCUS). It is effective for heavy-oil recovery.	CO_2 transportation and injection are costly. This technique requires a sealed reservoir to prevent gas leakage. It may cause equipment corrosion.	Average cost: USD 20–60 per additional barrel of oil. It is highly profitable when CO_2 infrastructure is available. Additional costs: it requires expensive compressors and gas capture systems.	5.06

For thermal EOR, the stepwise heating of water up to 95 °C was applied. The highest obtained increase in displacement efficiency was 17%. However, after 70 °C, the displacement efficiency increase declined, which may be attributed to the rheological properties of fluids: at temperatures above 70 °C, the viscosities of oil and water, as well as their viscosity ratios, change insignificantly.

The gas EOR methods led to lower improvements in the displacement efficiency. Filtration experiments on unconsolidated Cretaceous core samples from the East Moldabek field demonstrated that nitrogen injection led to a slight increase in the displacement efficiency, amounting to approximately 3%. CO_2 injection resulted in a displacement efficiency increase of 5.06% compared to conventional water flooding. This is due to the dissolution of the CO_2 in the oil, a process that reduces the viscosity and improves the mobility of oil. Additional studies must be conducted to further evaluate the feasibility of this method. However, this experimental study highlights the effectiveness of nitrogen and CO_2 injection in enhancing oil recovery in Cretaceous formations and demonstrates the

value of integrating laboratory methods into EOR research. These results can serve as a foundation for future filtration experiments and further EOR investigations.

This study presents the results of core filtration experiments aimed at evaluating the displacement efficiency of and assessing methods for enhancing oil recovery. However, several limitations must be considered when interpreting the obtained data.

Firstly, the laboratory experiments were conducted on core samples, which do not fully replicate the complex in situ conditions of reservoirs, which include formation heterogeneity, thermo-baric effects, and chemical interactions with formation fluids. Secondly, this study was based on a limited number of core samples, potentially reducing the representativeness of the results for reservoirs with significant geological variability. Additionally, the duration of the experiments was constrained, preventing a comprehensive assessment of the long-term stability of the injected agents and their impacts on reservoir properties.

To improve the reliability and applicability of the findings, further research should focus on the following areas:

1. Conducting extended experiments that consider cyclic injection and the potential retention of injected agents within the reservoir matrix;
2. Scaling up this study through field pilot tests and numerical simulations;
3. Investigating the impact of reservoir heterogeneity on displacement efficiency;
4. Developing more precise mathematical models of filtration processes;
5. Evaluating the environmental and economic feasibility of employing the studied technologies.

Advancing research in these directions will enable a more accurate adaptation of enhanced oil recovery (EOR) technologies to field-specific conditions and improve their industrial applicability.

Author Contributions: Conceptualization, K.S. and U.Z.; methodology, U.Z., K.S. and G.R.; investigation, K.S., U.Z. and Z.K.; data curation, K.S.; writing—original draft preparation, K.S. and G.R.; visualization, K.S.; supervision, G.R.; project administration G.R.; funding acquisition, G.R. All authors have read and agreed to the published version of the manuscript.

Funding: This research was funded by the Committee of Science of the Ministry of Science and Higher Education of the Republic of Kazakhstan (Grant No. AP19677859).

Data Availability Statement: The original contributions presented in this study are included in the article; further inquiries can be directed to the corresponding authors.

Acknowledgments: The authors would also like to express their gratitude to JSC "Embamunaigas" for providing data on the East Moldabek field section and to the LLP Atyrau Branch of "KMG Engineering" for their collaboration in conducting the filtration experiments.

Conflicts of Interest: Author Zhenis Kuatov was employed by the company Atyrau Branch of LLP "KMG Engineering". The remaining authors declare that the research was conducted in the absence of any commercial or financial relationships that could be construed as a potential conflict of interest.

Abbreviations

The following abbreviations are used in this manuscript:

EOR	Enhanced oil recovery
ASP	Alkaline-surfactant polymer
SAGD	Steam-assisted gravity drainage
WAG	Water alternating gas
HPAM	Partially hydrolyzed polyacrylamide

References

1. Liu, Z.; Yan, L.; Wang, Q.; Guo, Y.; Gao, M.; Wang, Z.; Liu, W. Status and progress of worldwide EOR field applications. *J. Pet. Sci. Eng.* **2020**, *193*, 107449. [CrossRef]
2. McGlade, C.; Sondak, G.; Han, M. *Whatever Happened to Enhanced Oil Recovery?* International Energy Agency: Paris, France, 2018.
3. Alvarado, V.; Manrique, E. Enhanced Oil Recovery: An update review. *Energies* **2010**, *3*, 1529–1575. [CrossRef]
4. Manrique, E.; Muci, V.E.; Gurfinkel, M. EOR field experiences in carbonate reservoirs in the United States. *SPE Reserv. Eval. Eng.* **2007**, *10*, 667–686. [CrossRef]
5. Advanced Resources International, Inc. *The U.S. CO_2 Enhanced Oil Recovery Survey*; Advanced Resources International, Inc.: Arlington, VA, USA, 2021.
6. Tarco, J.A.; Arteaga, G.R.; Merino, S.; Achig, J.M.; Estrella, J.M. Identification of Enhanced Oil Recovery Potential in Ecuador. In Proceedings of the SPE Latin American and Caribbean Petroleum Engineering Conference, Quito, Ecuador, 18–20 November 2015. [CrossRef]
7. Chen, P.; Balasubramanian, S.; Bose, S.; Alzahabi, A.; Thakur, G. An Integrated Workflow of IOR/EOR Assessment in Oil Reservoirs. In Proceedings of the Offshore Technology Conference, Houston, TX, USA, 30 April–3 May 2018. [CrossRef]
8. Meng, X.; Zhou, H.B.; Luo, D.K. Screening, Assessing, and Sorting Chinese Oilfields for CO_2-EOR Suitability and Potential Economic and Social Benefits. In Proceedings of the SPE/IAEE Hydrocarbon Economics and Evaluation Symposium, Houston, TX, USA, 17–18 May 2016. [CrossRef]
9. Vishnumolakala, N.; Zhang, J.; Ismail, N.B. A Comprehensive Review of Enhanced Oil Recovery Projects in Canada and Recommendations for Planning Successful Future EOR projects. In Proceedings of the SPE Canada Heavy Oil Conference, Virtual, 28 September 2020. [CrossRef]
10. Babadagli, T. Philosophy of EOR. In Proceedings of the SPE/IATMI Asia Pacific Oil & Gas Conference and Exhibition, Bali, Indonesia, 29–31 October 2019. [CrossRef]
11. Hartono, A.D.; Hakiki, F.; Syihab, Z.; Ambia, F.; Yasutra, A.; Sutopo, S.; Efendi, M.; Sitompul, V.; Primasari, I.; Apriandi, R. Revisiting EOR Projects in Indonesia through Integrated Study: EOR Screening, Predictive Model, and Optimization. In Proceedings of the SPE/IATMI Asia Pacific Oil & Gas Conference and Exhibition, Jakarta, Indonesia, 17–19 October 2017. [CrossRef]
12. Gbadamosi, A.; Junin, R.; Manan, M.A.; Yusuff, A.S. An overview of chemical enhanced oil recovery: Recent advances and prospects. *Int. Nano Lett.* **2019**, *9*, 171–202. [CrossRef]
13. Joshi, D.; Maurya, N.K.; Mandal, A. Evaluation of Synergetic Rheological Behaviour of Polymer and Silica Nanofluids for Enhanced Oil Recovery. In Proceedings of the SPE Annual Technical Conference and Exhibition, San Antonio, TX, USA, 16–18 October 2023. [CrossRef]
14. Al Shahri, H.; Liu, J.; Liu, K.; Clennell, M.B. Investigation of ASP Flooding Efficiency on Artificial Sandstone Cores: Homogenous Case. In Proceedings of the SPE EOR Conference at Oil & Gas West Asia, Muscat, Oman, 11–13 April 2010. [CrossRef]
15. Guo, H.; Dong, J.; Wang, Z.; Liu, H.; Ma, R.; Kong, D.; Wang, F.; Xin, X.; Li, Y.; She, H. 2018 EOR Survey in China-Part 1. In Proceedings of the SPE Improved Oil Recovery Conference, Tulsa, OK, USA, 14–18 April 2018. [CrossRef]
16. Sedighi, M.; Aminian, M.; Mohammadi, M.; Koohi, A.D. Overview of thermal concepts in enhanced oil recovery. In *Enhanced Oil Recovery: Methods, Challenges and Impacts*; Elsevier: Amsterdam, The Netherlands, 2023; pp. 1–45. [CrossRef]
17. Abdulkadir, U.; Hashim, J.; Alkali, M.; Kumar, A. Application of thermal methods for heavy oil recovery: Phase One. *Int. J. Adv. Res. Dev.* **2017**, *2*, 102–120.
18. Khalilnezhad, A.; Rezvani, H.; Abdi, A.; Riazi, M. Hybrid thermal chemical EOR methods. In *Enhanced Oil Recovery: Methods, Challenges and Impacts*; Elsevier: Amsterdam, The Netherlands, 2023; pp. 269–314. [CrossRef]
19. Ramey, H.; Brigham, W. A review of thermal recovery applications in the United States. In *Thermal Recovery*; Elsevier: Amsterdam, The Netherlands, 1977; pp. 591–609. [CrossRef]
20. Mokheimer, E.M.A.; Hamdy, M.S.; Abubakar, Z.; Shakeel, M.R.; Habib, M.A.; Mahmoud, M. A Comprehensive Review of Thermal Enhanced Oil Recovery: Techniques Evaluation. *J. Energy Resour. Technol.* **2018**, *141*, 030801. [CrossRef]
21. Ahmadi, M.A. Electromagnetic heating processes for heavy oil and bitumen recovery. In *Enhanced Oil Recovery: Methods, Challenges and Impacts*; Elsevier: Amsterdam, The Netherlands, 2023; pp. 359–397. [CrossRef]
22. Pothula, G.K.; Vij, R.K.; Bera, A. An overview of chemical enhanced oil recovery and its status in India. *Pet. Sci.* **2023**, *20*, 2305–2323. [CrossRef]
23. Jain, A.K.; Dhawan, A.K.; Misra, T.R. ASP Flood pilot in Jhalora (K-IV)—A case study. In Proceedings of the SPE Oil and Gas India Conference and Exhibition, Mumbai, India, 28–30 March 2012. [CrossRef]
24. Tiwari, D.; Marathe, R.V.; Patel, N.K.; Ramachandran, K.P.; Maurya, C.R.; Tewari, P. Performance of polymer flood in Sanand Field, India-A case study. In Proceedings of the SPE Oil and Gas India Conference and Exhibition, Perth, Australia, 20–22 October 2008. [CrossRef]
25. Lwisa, E.G. Chemical enhanced oil recovery. *Int. J. Innov. Educ. Res.* **2021**, *9*, 160–172. [CrossRef]

26. Zwaan, M.; Valdez, R. Chemical and Miscible Gas EOR Field Development Strategies Based on Integrated Surveillance Interpretation. In Proceedings of the SPE Kuwait Oil and Gas Show and Conference, Mishref, Kuwait, 11–14 October 2015. [CrossRef]
27. Koyanbayev, M.; Wang, L.; Wang, Y.; Hashmet, M.R. Advances in sour gas injection for enhanced oil recovery-an economical and environmental way for handling excessively produced H_2S. *Energy Rep.* **2022**, *8*, 15296–15310. [CrossRef]
28. Zhang, F.; Adel, I.A.; Saputra, I.W.; Chen, W.; Schechter, D.S. Numerical Investigation to Understand the Mechanisms of CO_2 EOR in Unconventional Liquid Reservoirs. In Proceedings of the SPE Annual Technical Conference and Exhibition, Calgary, AB, Canada, 30 September–2 October 2019. [CrossRef]
29. Zhapbasbayev, U.K.; Kudaibergenov, S.E.; Mankhanova, A.; Sadykov, R. Experimental study of alkaline-surfactant-polymer compositions for ASP-flooding of cores from highly viscous oil reservoirs. *Thermophys. Aeromech.* **2018**, *25*, 909–916. [CrossRef]
30. Abirov, R.; Ivakhnenko, A.P.; Abirov, Z.; Eremin, N.A. The associative polymer flooding: An experimental study. *J. Pet. Explor. Prod. Technol.* **2019**, *10*, 447–454. [CrossRef]
31. Abdurrahman, M. Chemical enhanced oil recovery (EOR) activities in Indonesia: How it's future. *AIP Conf. Proc.* **2017**, *1840*, 090003. [CrossRef]
32. Musayev, M.S.; Musharova, D.; Zhappasbayev, B.; Orynbassar, E.K. The experience of implementation of polymer flooding technology at Zaburunye oil filed as a method for developing mature fields. *Vestn. Neftegazovoj Otrasli Kaz.* **2021**, *3*, 29–42. [CrossRef]
33. Dong, X.; Liu, H.; Chen, Z.; Wu, K.; Lü, N.; Zhang, Q. Enhanced oil recovery techniques for heavy oil and oilsands reservoirs after steam injection. *Appl. Energy* **2019**, *239*, 1190–1211. [CrossRef]
34. Mankhanova, A.; Ogay, Y.K.; Zolotukhin, A.; Zhapbasbayev, U.K. Selection of the effective enhanced oil recovery method for highly viscous oil fields on the basis of filtration experiments (on the example of one Kazakhstani field). In Proceedings of the SPE Oil and Gas India Conference and Exhibition, Astana, Kazakhstan, 12–14 November 2014. [CrossRef]
35. Hou, Q.; Guo, D.; Ouyang, J. Laboratory Study on Switchable Alkylamidine Surfactant for Daqing Oilfield. In Proceedings of the International Petroleum Technology Conference, Bangkok, Thailand, 14–16 November 2016. [CrossRef]
36. Singh, B.P.; Parulkar, S.; Kumar, A. Successful Pilot Implementation of ASP Flooding through CEOR/IOR Application—A Case Study. In Proceedings of the SPE Oil and Gas India Conference and Exhibition, Mumbai, India, 4–6 April 2017. [CrossRef]

Disclaimer/Publisher's Note: The statements, opinions and data contained in all publications are solely those of the individual author(s) and contributor(s) and not of MDPI and/or the editor(s). MDPI and/or the editor(s) disclaim responsibility for any injury to people or property resulting from any ideas, methods, instructions or products referred to in the content.